

523-47
197523
p-5

1994017842

N 9 4 - 2 2 3 1 5

CIRRUS CLOUD RETRIEVALS FROM HIS OBSERVATIONS DURING FIRE II

S. A. Ackerman, W. L. Smith, X. L. Ma, R. O. Knuteson and H. E. Revercomb

ABSTRACT

This paper presents 1) retrieval methods applied to HIS observations during FIRE II and 2) doubling/adding model developed to simulate high-spectral resolution infrared radiances in a cloudy atmosphere. The capabilities of the retrieval methods and sensitivity studies of high-altitude aircraft based observations to cloud microphysical structure are conducted with the model.

OBSERVATIONS

Methods of detecting cirrus clouds and inferring their radiative properties have been developed at the University of Wisconsin-Madison under the High-resolution Interferometer Sounder (HIS) program (e.g., Smith and Frey, 1990; Ackerman et al, 1990; and Smith et al, 1993). The HIS instrument is a calibrated nadir viewing Michelson interferometer which flies on board the NASA high altitude ER-2 aircraft. Figure 1 is an example of the retrieved cloud pressure altitude using the CO₂ slicing method developed for high-spectral resolution observations (Smith and Frey 1990) for the period 17:50 to 18:04 UTC on December 5. The white line is the retrieved cloud altitude and the dark line the IR window equivalent blackbody temperature. Dotted lines indicate the HIS in its calibration mode or no cloud height retrieval. The HIS time series is overlain the CALS lidar image, provide by Dr. J. Spinhirne. While the CO₂ slicing method is detecting the presence of the cloud, its effective altitude varies more than the lidar observed cloud. The cloud is very inhomogeneous, making it a difficult situation for any cloud retrieval technique. We are employing model simulations to test the sensitivity of the CO₂ slicing method, and other cloud retrieval techniques, to cloud microphysical properties (this will be presented at the conference). Figure 2 depicts the tri-spectral approach to detecting cirrus cloud (Ackerman et al 1990) for the same period as Figure 1. Positive 8.3-11 μm brightness temperature differences are indicative of cloud. We are combing the tri-spectral technique with the CO₂ slicing technique and the cloud emissivity techniques of Ackerman et al (1990) and Smith at al (1993) to improve the detection of cirrus cloud and the retrieval of its radiative properties.

MODEL SIMULATIONS

Infrared observations at a spectral resolution of 1 cm⁻¹, or finer, have proven to be extremely valuable in assessing line-by-line radiative transfer models and in retrieving atmospheric temperature and moisture profiles (Smith et al 1989). Techniques have also been developed to infer, in cloudy sky atmospheric conditions, cloud radiative properties in addition to temperature and moisture profiles from the high spectral resolution observations. To develop, verify and test these cloud retrieval techniques requires accurate simulations of observed radiances. These model based simulations have to accurately account for multiple scattering by the cloud layer, as well as emission and absorption of the gases in the atmosphere.

Assuming a plane-parallel horizontally homogeneous cloud, the IR radiative transfer equation is

$$\mu \frac{dI(\delta, \mu)}{d\delta} = I(\delta, \mu) - (1 - \omega_0)B(T) - \frac{\omega_0}{2} \int_{-1}^1 P(\delta, \mu, \mu') I(\delta, \mu') d\mu'$$

where $I(\delta, \mu)$ is the azimuthally average monochromatic intensity, δ is the optical thickness, ω_0 is the single scattering albedo, $P(\delta, \mu, \mu')$ is the azimuthally averaged phase function, $B(T)$ represents the Planck function at temperature T , and $\mu = \cos \theta$ where θ is measured from the downward normal direction. An accurate numerical technique to solve equation (1) is the doubling/adding method which has been discussed in detail in previous atmosphere studies (Grant and Hunt, 1969; Wiscombe 1976; Wiscombe and Grams 1976; Wiscombe and Evans 1977, Stephens 1980).

For the purposes of this paper, we have assumed the cloud is composed of spherical ice particles distributed according to a modified gamma distribution. Scattering is neglected in the clear sky atmosphere so that, for a single cloud layer, the atmosphere is divided into three layers: above, within and below the cloud layer. Radiances and transmittances in the clear sky conditions are determined from FASCOD3 calculations. The incident radiances at the cloud boundaries must be specified. Rather than

run separate FASCOD3 calculations for each angle incident on the cloud, for the purposes of this paper, FASCOD3 is used to the nadir and zenith angle radiance, the angular distribution is derived by weighting the FASCOD3 radiance by the cosine of the incident angle. FASCOD3 is used to assign gaseous transmittance within the cloud.

Examples of model simulations which correspond to conditions observed during the coincident FIRE II Cirrus and SPECTRE field experiments, will be presented at the conference. Vertical profiles of temperature, moisture and ozone were measured during 5 December 1991. Both ground based and ER-2 based observations were also available during this time period. Lidar observations indicated a cirrus cloud between approximately 10 and 12.3 km. The model discussed above was used to simulate high-spectral resolution observations for a variety of assumed cloud microphysical properties. Here we want to briefly highlight the sensitivity of the observations to different microphysical properties.

An example of the sensitivity of the HIS observations to ice water path (IWP) is depicted in Figure 3. The reference spectra is computed for a cloud with $IWP=6.9 \text{ g/m}^2$, an effective radius of $30 \mu\text{m}$ and a variance of 0.25. In each subsequent calculation, only the IWP was changed (values are: 0.23, 0.69, 1.61, 2.3, 16.1, 23., 69., and 161 g/m^2). Differences between the different IWP's are depicted in terms of the difference in equivalent brightness temperature from the reference spectra (ΔBT). Negative values indicate a larger IWP and positive values a smaller IWP. As expected the more opaque the band the less sensitivity to IWP and the cloud in general. Maximum sensitivity occurs in the regions between absorptance lines. For these high clouds, the aircraft based instrument has more sensitivity to the cloud IWP in the spectral regions $500\text{-}600 \text{ cm}^{-1}$ and $1300\text{-}1500 \text{ cm}^{-1}$. Water vapor absorption is dominant in these spectral regions, the majority of which lies between the surface and the cloud base obscuring the view of the cloud from the ground-based instrument. In the region $1100\text{-}1300 \text{ cm}^{-1}$, the ER-2 view sees a constant ΔBT , at least in-between absorption lines. For the spectral region $850\text{-}1000 \text{ cm}^{-1}$, the ΔBT is spectrally dependent. The spectral variation of ΔBT depends on the IWP though it is less than approximately 2° . This spectral variation in BT is driven by the spectral variation in the cloud optical properties and therefore rooted to the cloud particle size distribution.

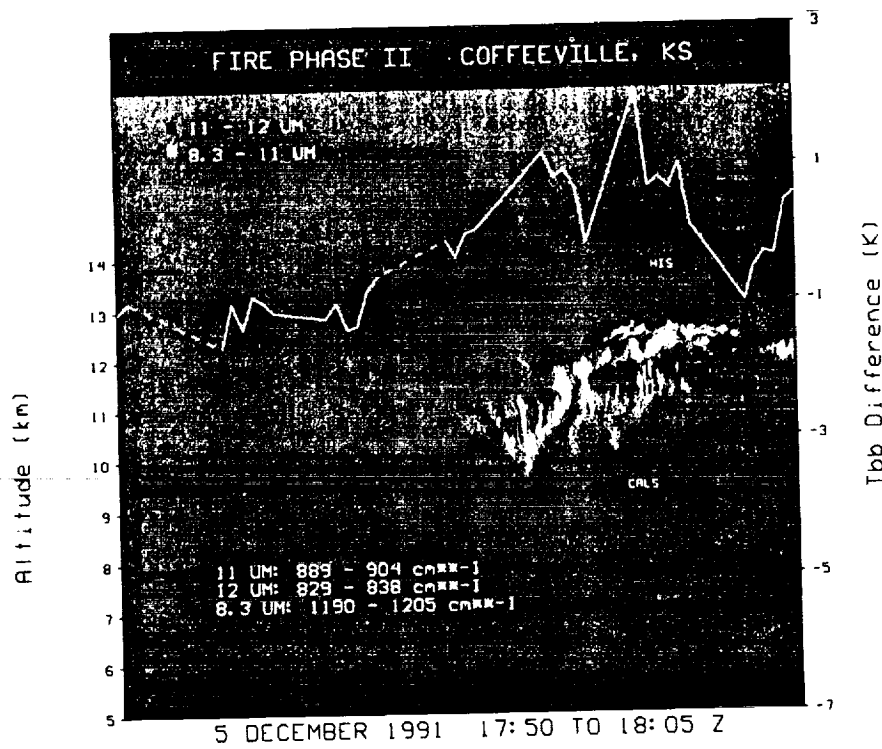
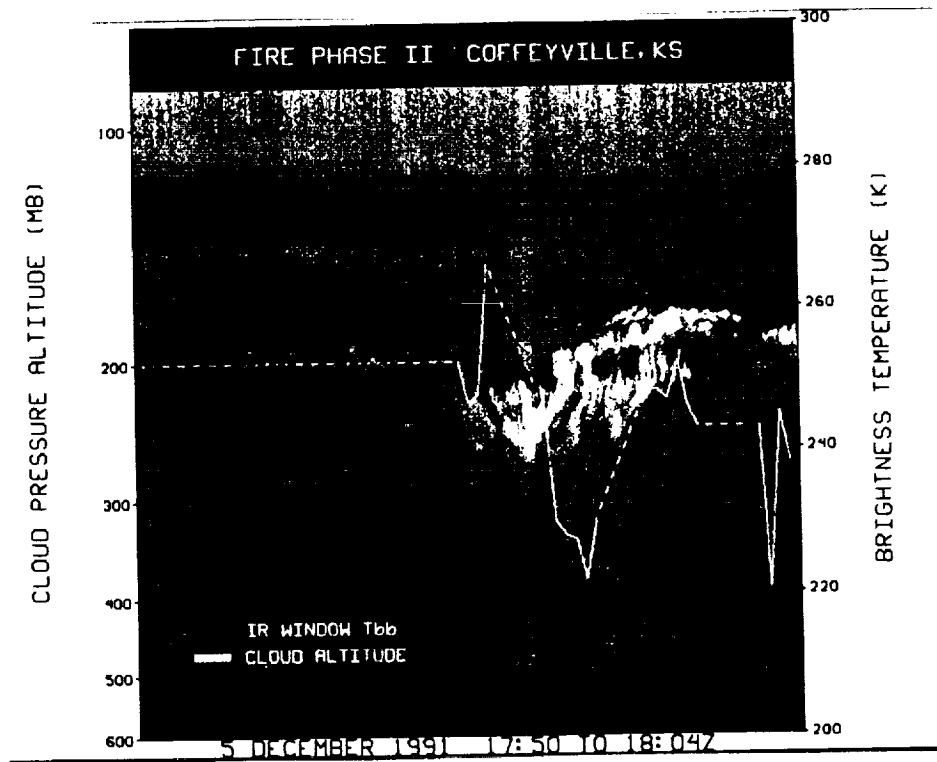
Sensitivity of the simulated spectre to changes in cloud particle size distribution are depicted in figure 4. Again results are displayed in terms of the brightness temperature difference from a reference spectra. The reference spectra has a particle size distribution with $a=30 \mu\text{m}$ and a variance of $b=0.25$; comparison are made for small effective radius ($a=15\mu\text{m}$) and larger effective radius ($a=120\mu\text{m}$). Comparisons were conducted for three equivalent IWP's, .23, 2.3 and 23 g/m^2 . The positive ΔBT represent differences between the $30 \mu\text{m}$ effective radius distribution and the $15 \mu\text{m}$ distribution. As seen in Figure 4, the smaller the IWP the less difference between spectra with different effective radii. The scales were kept the same as the IWP comparison to demonstrate the dominating effect of the cloud ice water path. The spectral region that appears to be most sensitive to particle size is the $950\text{-}1050 \text{ cm}^{-1}$ ($>5^\circ$). Variations in this spectral regime are larger than the IWP dependence. The magnitude depends on the IWP, while the particle size controls the shape of the ΔBT curve.

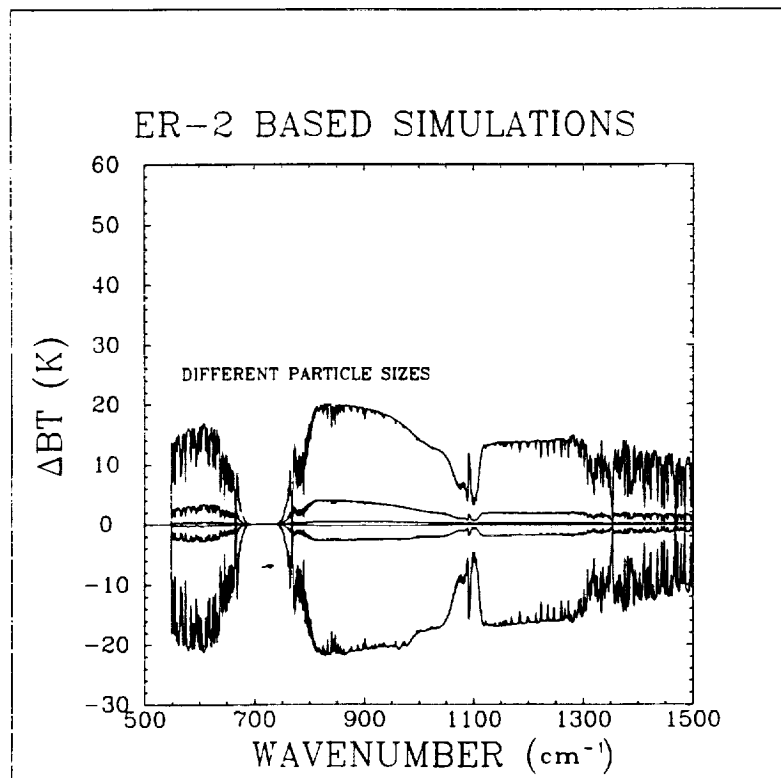
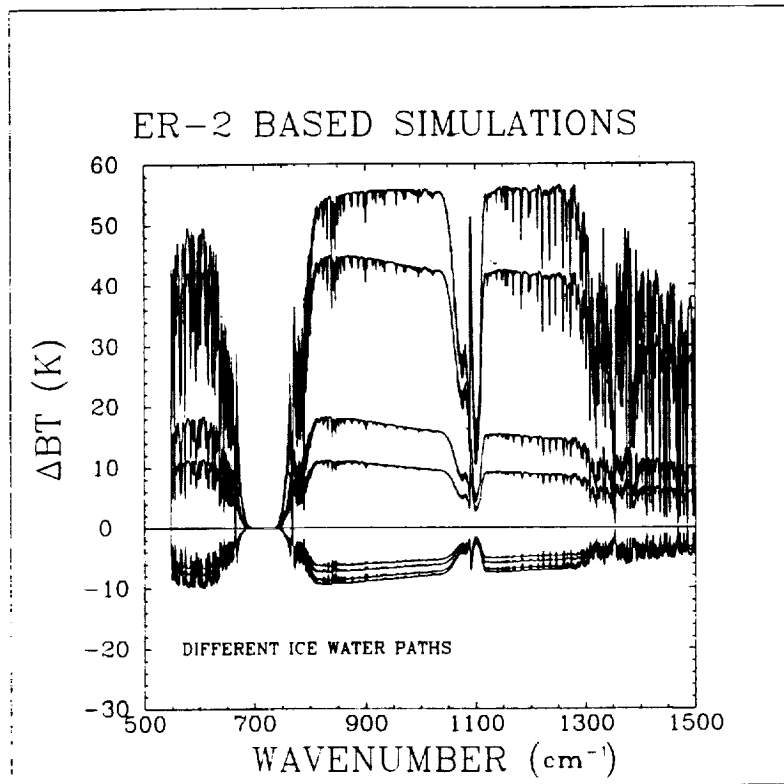
Further sensitivity studies and data analysis will be presented at the meeting.

REFERENCES

- Ackerman, S. A., W. L. Smith, J. D. Spinhirne, and H. E. Revercomb, 1990: The 27-28 October 1986 FIRE cirrus case study: spectral properties of cirrus clouds in the $8\text{-}12 \mu\text{m}$ window. *Mon. Wea. Rev.*, **118**, 2377-2388.
- Revercomb, H.E., H. Buijs, H.B. Howell, D.D. LaPorte, W.L. Smith, and L.A. Sromovsky, 1988: Radiometric Calibration of IR Fourier Transform Spectrometers: Solution to a Problem with the High Resolution Interferometer Sounder. *Applied Optics*, **27**, 3210-3218.
- Smith W. L., H. E. Revercomb, D. D. LaPorte, H. M. Woolf, H. B. Howell, R. O. Knuteson, H. L. Huang, L. A. Sromovsky and S. Silverman, 1989: GHIS, the Geostationary High-resolution Interferometer Sounder. *CIMSS View*, Vol. V, No.1, available from the Space Science and Engineering Center, University of Wisconsin, Madison, Wisconsin, 53706.
- Smith W.L., Xia Lin Ma, S.A. Ackerman, H.E. Revercomb, and R.O. Knuteson, 1993: Remote Sensing Cloud Properties from High Spectral Resolution Infrared Observations. *J. Appl. Met.*, in press, 1993.

Smith, W. L. and R. Frey, 1990: On cloud altitude determinations from high resolution interferometer sounder (HIS) observations. *J. Appl. Meteor.*, 29, 658-662.





REFERENCES

Ackerman, S. A., W. L. Smith, J. D. Spinhurne, and H. E. Revercomb. 1990: The 27-28 October 1986 FIRE cirrus case study: spectral properties of cirrus clouds in the 8-12 μm window. *Mon. Wea. Rev.*, **118**, 2377-2388.

Revercomb, H.E., H. Buijs, H.B. Howell, D.D. LaPorte, W.L. Smith, and L.A. Sromovsky. 1988: Radiometric Calibration of IR Fourier Transform Spectrometers: Solution to a Problem with the High Resolution Interferometer Sounder. *Applied Optics*, **27**, 3210-3218.

Smith W. L., H. E. Revercomb, H. B. Howell, and M. -X. Lin: 1988: Multi-spectral window radiance observations of cirrus from satellite and aircraft - November 2, 1986 "Project FIRE", *FIRE Science Results 1988*, Proceeding of a conference held in Vail, CO July 11-15, pp 89-93.

Smith W. L., H. E. Revercomb, D. D. LaPorte, H. M. Woolf, H. B. Howell, R. O. Knuteson, H. L. Huang, L. A. Sromovsky and S. Silverman, 1989: GHIS, the Geostationary High-resolution Interferometer Sounder. *CIMSS View*, Vol. V, No.1, available from the Space Science and Engineering Center, University of Wisconsin, Madison, Wisconsin. 53706.

Smith W.L., Xia Lin Ma, S.A. Ackerman, H.E. Revercomb, and R.O. Knuteson, 1993: Remote Sensing Cloud Properties from High Spectral Resolution Infrared Observations. *J. Appl. Met.*, in press, 1993.

Smith, W. L. and R. Frey, 1990: On cloud altitude determinations from high resolution interferometer sounder (HIS) observations. *J. Appl. Meteor.*, **29**, 658-662.

Smith, W. L., and R. Frey, 1991: Altitude specification of cloud motion winds. Workshop on Wind Extraction from Operational Meteorological Satellite Data, Washington, D.C. September 17-19.

Table 2. WISCONSIN AERI INSTRUMENT OPERATIONS

LOCATION: COFFEYVILLE, KANSAS
 YEAR: 1991
 REMARKS: (1) Observations are at 10 minute intervals between stated START and END times. (2) The letter H indicates that the ER-2 HIS was overhead. (3) OP # refers to an AERI operating period.

OP #	DATE	TIME PERIOD	CONDITIONS FROM VISUAL OBS
1	11 NOV	17:06 - 17:30	low overcast
2	12 NOV	23:26 - 02:29	cirrus
	13 NOV	02:53 - 04:28	cirrus/clear
3	13 NOV	18:18 - 01:26	cirrus
	14 NOV	02:13 - 03:41	thin cirrus
4	17 NOV	17:58 - 21:12	mixed cirrus to clear
	18 NOV	01:29 - 24:00	clear
	19 NOV	00:00 - 05:57	clear/cirrus/low thick cloud
5	20 NOV	17:20 - 23:33	clear
	21 NOV	00:12 - 24:00	clear
	22 NOV	00:00 - 19:07	cirrus/clear/rain
6	23 NOV	16:28 - 24:00	clear/mixed/overcast
	24 NOV	00:47 - 23:29	overcast/clear
	25 NOV	00:37 - 05:48	overcast
7	25 NOV	16:19 - 23:52	alto-cumulus/scatter cirrus
	26 NOV	00:29 - 24:00	clear/cirrus/mixed
8	27 NOV	14:01 - 17:21	low cloud
9	28 NOV	14:40 - 22:35	cirrus/overcast stratus
10	29 NOV	15:00 - 24:00	overcast/clear
	30 NOV	00:00 - 17:34	clear/overcast
11	03 DEC	00:25 - 23:08	overcast/ clear/ cold
	04 DEC	23:55 - 06:41	clear
12	04 DEC	17:16 - 24:36	clear/ aerosol
	05 DEC	01:23 - 24:00	clear/cirrus
	06 DEC	00:00 - 05:31	thin cirrus
13	06 DEC	14:52 - 20:33	mixed cirrus/alto cu
	07 DEC	00:54 - 05:52	clear/ aerosol/low cloud
14	07 DEC	14:49 - 21:23	low overcast/broken low